What Determines Inhomogeneous Broadening of Electronic Transitions in Conjugated Polymers?

Sebastian T. Hoffmann, Heinz Bässler, and Anna Köhler*

Experimentalphysik II, Universität Bayreuth, Bayreuth

Received: August 5, 2010; Revised Manuscript Received: November 8, 2010

Energetic disorder is manifested in the inhomogeneous broadening of optical transitions in π-conjugated organic materials, and it is a key parameter that controls the dynamics of charge and energy transfer in this promising class of amorphous semiconductors. In an endeavor to understand which processes cause the inhomogeneous broadening of singlet and triplet excitations in π-conjugated polymers we analyze continuous wave absorption and photoluminescence spectra within a broad range of temperatures for (i) oligomers of the phenylenevinylene family (OPVs) and MEH-PPV in solution and (ii) bulk films of MEH-PPV and members of the poly(*p*-phenylene) family (PPPs). We use a Franck−Condon deconvolution technique to determine the temperature dependent S_1-S_0 0−0 and T_1-S_0 0−0 transition energies and their related variances. For planar compounds, the transition energies can be related to the oligomer length, which allows us to infer the effective conjugation length for the nonplanar compounds as a function of temperature. With this information we can distinguish between intrachain contributions to the inhomogeneous line broadening that are due to thermally induced torsional displacements of the chain elements, and other contributions that are assigned largely to dielectric interactions between the chain and its environment. We find that in solution, temperature-induced torsional displacements dominate the line broadening for the alkyl derivatives of OPVs while in the alkoxy derivatives the Van der Waals contribution prevails. In films, σ is virtually temperature independent because disorder is frozen in. We also establish a criterion regarding the ratio of inhomogeneous line broadening in singlet and triplet states. The results will be compared to a recent theory by Barford and Trembath.

1. Introduction

The distribution of excited states is a fundamental property of an ensemble of chromophores constituting an organic semiconductor. It controls the absorption, the fluorescence, and the phosphorescence spectra, as well as interactions among the chromophores. Manifestations of the latter are charge and energy transfer that are of paramount importance for the operation of optoelectronic devices.[1−3] Understanding the underlying mechanisms that contribute to the density of states distribution is therefore a timely challenge toward designing materials with improved structure−property relations.

The optical spectroscopy of organic compounds is dominated by transitions among excitonic singlet and triplet states that couple to molecular vibrations. In materials that lack translational symmetry, i.e., fluid or solid solutions, molecularly doped polymers, or neat polymers, optical transitions are inhomogeneously broadened. This is a signature of disorder that can be of variable origin. For example, in a dense system, an optical transition dipole couples to the induced dipoles in the surrounding medium. This is a Van der Waals type polarization effect that causes the shift between the energies of the excited chromophore in the gas phase and the medium. Since the coupling strength depends on many internal parameters and thus obeys a random statistic, the profile of the resulting inhomogeneously broadened transition is of a Gaussian shape.[4] Line broadening can further be enhanced by randomly oriented permanent dipoles in the environment.[5−7] A similar Van der Waals type polarization effect occurs when an electron is added to or removed from a chromophore. In this case it is the energy level of the ionic species that is inhomogeneously broadened.[8,9] Unfortunately, in organic media, direct transitions from the ground state to ionized states are not amenable to optical spectroscopy but are revealed in an indirect way by studies on charge transport, for instance, in molecularly doped polymers used in electrophotography.[10] Typically, the variance of the density of states (DOS) distribution of charge transporting states is about 100 meV but is about 50 meV for excitonic states, with larger values for singlets than for triplets.[8] However, one should be aware that in a fluid system the Van der Waals coupling of an excited chromophore is a dynamic property because of time and temperature dependent solvation. If the solvent shell next to the chromophore changes upon excitation, this can have a feedback effect on the inhomogeneous line broadening and, concomitantly, on the Stokes' shift between absorption and emission.[11]

In addition to the intermolecular contribution to the inhomogeneous line broadening discussed so far, an intramolecular element can arise from the conformational disorder of a chromophore. This occurs for example in π-conjugated polymers. The general notion is that a polymer can be considered as a chain of chromophores comprising a statistically varying number of repeat units.[12−17] Since electronic coupling between chromophores is weaker than the coupling within the chromophore, the electronic excitations behave like a particle in a box whose energy levels depend on the length of the box. The so-called conjugation length or, synonymously, the electronic persistence length that defines the chromophore is limited mainly by conjugation breaks and/or by torsional displacements of the repeat units such as thiophene or phenylene rings, though other effects have also recently been suggested.[18,19]

* Corresponding author. E-mail: anna.koehler@uni-bayreuth.de.

10.1021/jp107357y
Published on Web 12/07/2010

The purpose of the present work is to identify spectroscopically the origin of disorder in π-conjugated polymers and to distinguish between the relative contribution from intrachain torsions and that from other effects, mainly by the polarization of the environment. In our study we apply continuous wave (cw) absorption and photoluminescence spectroscopy. Absorption provides snapshots of the momentary density of states during optical excitation while photoluminescence probes the excitation after chain relaxation to a quasi static state is completed. To monitor the temporal course of chain relaxation would require time-resolved or even ultrafast detection techniques.[20−24] Note, however, that the time averaged, quasi-static density of states is the relevant parameter that controls energy and charge transfer in π-conjugated films because the rates of interchain charge and energy exchange are usually much lower than intrachain structural relaxation.[23,25]

The present work was stimulated by the theoretical treatment of disorder of a poly(*p*-phenylene) chain by Barford and Trembath.[18] They investigated the temperature dependence of inhomogeneous line broadening for singlet and triplet excitons on a poly(*p*-phenylene). In their approach, they differentiate between thermally induced static disorder due to torsional displacements and the static effect of the polarization of the environment. The torsionally induced intrachain contribution is included by considering a parametrized biphenyl torsion potential, while the Van der Waals contribution is included by embedding the chromophore in a dielectric medium. Not included in the theory are, first, impediments to torsions on the chromophore, e.g., by interactions between the side chains of the chain and its environment and, second, structural dynamics of the environment such as solution or glass dynamics. The authors found that there is a correlation between the conformational disorder and the conjugation length defined as the spread of the center of mass wave functions of the (two-particle) exciton.[18,26] Among the results are the predictions

(i) that the inhomogeneous line width in solution scales with $T^{2/3}$ where T is the absolute temperature. (Note that for a given disorder σ the inhomogeneous line width of absorption scales with $\sigma^{4/3}$ in their model.[19] In ref 18, Barford and Trembath find that the disorder depends on temperature as $\sigma \sim T^{1/2}$, implying a corresponding dependence of the absorption line width as $\sim T^{2/3}$).

(ii) that the triplet excitons are more spatially localized than singlets, and furthermore that the relative off-diagonal disorder in absorption due to torsions is larger for triplets than for singlets.

(iii) that the absorption line width is roughly on the order of 0.5 eV.

To probe whether the theory of Barford and Trembath is applicable to materials in the solid state or in solution, we experimentally studied the inhomogeneous line broadening in oligomeric and polymeric π-conjugated systems in both solution and bulk films over a broad temperature range. We quantitatively distinguish the various contributions to disorder and compare the temperature dependent line broadening in rigid systems to that in systems in which torsional motions can be important. When comparing the predictions by Barford and Trembath to the experimental results, we find that there are some issues that might be worth addressing in future work. For example, in fluid solution the inhomogeneous line broadening of absorption does increase with temperature, albeit with a slightly stronger temperature dependence than the predicted $T^{2/3}$. We also identify systems in which the line width of phosphorescence is the same or smaller than that in fluorescence. This is the opposite order of what is predicted by theory, though we note that the theoretical predictions are valid only for absorption, while the experimental data on triplets can only be gathered through emission measurements. Furthermore, the experimentally derived line widths, in particular the Van der Waals contribution, are lower than those predicted by the theory. The experimental results allow us to establish a consistent concept to account for disorder-induced line broadening in π-conjugated polymers.

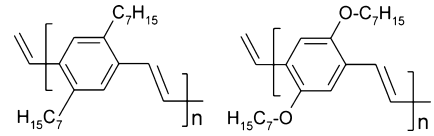

Figure 1. Structure of heptyl-OPVN (left) and heptoxy-OPVN (right). To take account of the extension of the π-electron distribution by the terminal vinylene groups, we characterize the length of the oligomers by the number N of vinyl bonds, with $N = n + 1$ where n is the number of phenylene−vinylene groups.

We consider three classes of materials: poly(*p*-phenylenevinylenes) (PPVs), poly(*p*-phenylenes) (PPPs), and a Pt-containing poly(*p*-phenyleneethylene). Our investigations focus on the PPVs. We analyze literature results on alkyl-[27] and alkoxy-substituted[28] phenylenevinylene oligomers (OPV*n*) and compare them with additional measurements we made on the polymer MEH-PPV in fluid solution, in solid solution, and in neat film. This is complemented with data obtained from published spectra on the PPPs and the Pt-polymer.[29]

2. Experimental Section

The analysis of absorption and fluorescence spectra of alkyl and alkoxy derivatives of oligomers of the phenylenevinylene family is based upon the work of Narwark et al.[27,28] They characterized a homologous series of metathetically synthesized, monodisperse all-trans oligomers of 2,5-diheptyl-*p*-divinylbenzene (heptyl-OPV*n*) and 2,5-(diheptyloxy)-*p*-divinylbenzene (heptoxy-OPV*n*) (Figure 1) by conventional absorption and cw fluorescence spectroscopy within a temperature range between 300 and 80 K. In most cases the solvent was methyltetrahydrofuoran (MeTHF). In the original work the n refers to the number of the phenylenevinylene rings. To account for fact that in metathetically synthesized oligomers there are two terminal vinylene groups that increase the size of the π-electron system, we shall label the oligomers as OPV*N* with $N = n + 1$. For example, OPV4 consists of four vinylene units separated by a total of three phenyl rings. This procedure will be justified by the successful parametrization of the dependence of the transition energy as a function of the chain length.

To complement the literature data, absorption and cw fluorescence were measured for films and solutions of MEH-PPV (poly(2-methoxy-5-((2-ethylhexyl)oxy)-1,4-phenylenevinylene)) and for solutions of MeLPPP (a ladder-type poly(*p*-phenylene)). The MEH-PPV was received from American Dye Sources Ltd. (ADS), Canada, while MeLPPP was provided by the group of Ulrich Scherf in Wuppertal after being synthesized as described in ref 30. Absorption measurements of MEH-PPV were taken in quartz cuvettes in MeTHF solution at a concentration of 5×10^{-6} mol/L. All other solution measurements shown were carried out at a concentration of 10^{-7} mol/L. The quantity "mol" refers to the individual repeat unit of the polymer. To prepare the thin film samples, MEH-PPV was spin-cast onto a quartz substrate from a MeTHF solution of about 15 mg/mL.

For the temperature dependent measurements of absorption or fluorescence, the cuvette or quartz substrate was placed in a continuous flow cryostat. The temperature was monitored using

a home-built temperature controller. At each temperature, we waited for 10−15 min to ensure a stable equilibrium temperature is obtained throughout the sample space. To acquire the absorption spectra, we excited using a tungsten lamp and recorded the transmission dispersed by a monochromator using a silicon diode and a lock-in amplifier. The spectra were corrected for the transmission of the setup. For the photoluminescence spectra, we excited at 405 nm (3.06 eV) using a diode laser and recorded the emission spectrum with a glass fiber connected to a spectrograph with a CCD camera attached (Oriel MS125 attached to Oriel Instaspect IV).

To obtain an accurate energetic position for the S_1-S_0 0−0 transition in absorption and emission, as well as to derive the correct variance σ of the line width, we deconvoluted the absorption and emission bands using a Franck−Condon analysis as described in refs 31−33. For example, to model the absorption spectrum $A(\hbar\omega)$ in the photons/energy interval, we used the expression[31−33]

$$A(\hbar\omega) = n^3(\hbar\omega)^3 \sum_{n_i} \prod_i \frac{e^{-S} S_i^{n_i}}{n_i}! \Gamma\delta[\hbar\omega - (\hbar\omega_0 + \sum n_i \hbar\omega_i)]$$

where $\hbar\omega_0$ is the energy of the 0−0 peak, $\hbar\omega_i$ are the vibrational energies of the modes i taken from Raman spectra, n_i denotes the number of vibrational overtones, Γ is the Gaussian Lineshape operator (kept at constant variance σ for all modes i and overtones n_i), and S_i is the Huang−Rhys parameter for the mode i. Γ is related to the variance σ of the line width by

$$\Gamma = \frac{1}{\sigma\sqrt{2\pi}} e^{-(\hbar\omega - \hbar\omega_0)^2/2\sigma^2}$$

n is the refractive index of the surrounding medium. The refractive index of MeTHF is 1.4 and can be considered constant over the range investigated, since MeTHF is transparent in this spectral range. We considered two modes i and $n_i = 4$ overtones for each mode. For a set of spectra recorded at different temperatures, the Huang−Rhys parameters S_i were kept constant while the position of the 0−0 transition and the variance σ of the Gaussian Lineshape operator were allowed to vary. The modes considered were 1306 cm^{-1} (C═C stretching coupled to C−H bending of the vinyl group) and 1586 cm^{-1} (C−C stretching of the phenyl ring) for MEH-PPV and OPVs[34] and 1295 cm^{-1} (aromatic ring C−C stretching vibration) and 1563 cm^{-1} (inter-ring stretching mode) for the PPPs.[31]

The density functional theory (DFT) calculations were carried out using the B3LYP hybrid functional together with the basis set 6-311G*. All DFT calculations were carried out with the Gaussian 09 program.

3. Results

Figure 2 shows the evolution of the absorption spectra of heptyl-OPV4 in MTHF solution upon cooling. These data are replotted from ref 27. The room temperature absorption spectra are broad and unstructured. Upon cooling, vibrational structure develops gradually and the absorption spectra shift toward lower energy. At 80 K, i.e., below the glass transition of MTHF, which is close to 90 K, there is a well-defined $S_1 \leftarrow S_0$ 0−0 transition. To quantify the spectral changes with temperature by the shift in the 0−0 energy and the broadening of the variation σ of the inhomogeneous line width, the vibrational structure of the spectra need to be deconvoluted. This is essential to obtain

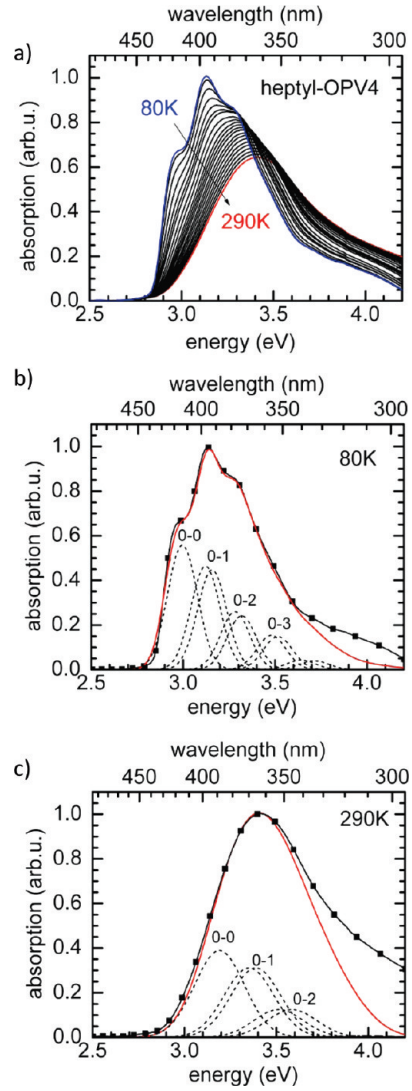

Figure 2. (a) Absorption spectra of heptyl-OPV4 recorded in MeTHF solution at different temperatures starting at 290 K in 10 K steps down to 80 K ($c = 4 \times 10^{-5}$ mol/L) (from ref 27). (b) and (c) show the Franck−Condon analyses of the spectra at 80 and 290 K, respectively. The experimental data are shown as black lines with squares; the fit is indicted as a red solid line. For illustration, the 0−0 peak as well as the first few overtones of the two vibrational modes involved in the progression are indicated as dotted lines. For clarity, linear combinations of overtones and higher overtones are omitted in the display, yet included in the fit.

the correct line width and energy. This deconvolution can be achieved using a Franck−Condon analysis making the plausible assumption that the spectra are built on the $S_1 \leftarrow S_0$ 0−0 transition with vibrational overtones that have temperature independent vibrational energies and a temperature independent Huang−Rhys factor. The only parameters considered to have a temperature dependence are the line width and, of course, the energetic position of the 0−0 transition. This is illustrated in Figure 2b,c, where the experimental absorption data are shown at 80 and 290 K along with a Franck−Condon fit comprising the 0−0 transition and four overtones of two vibrational modes. We use the same vibrational energies and Huang−Rhys factors for both temperatures, yet allow for different line width σ and energetic position of the 0−0. This analysis shows that, for the room temperature spectra, neither is the maximum of the absorption spectrum a measure of the $S_1 \leftarrow S_0$ 0−0 transition energy nor does the spectral width reflect the correct inhomo-

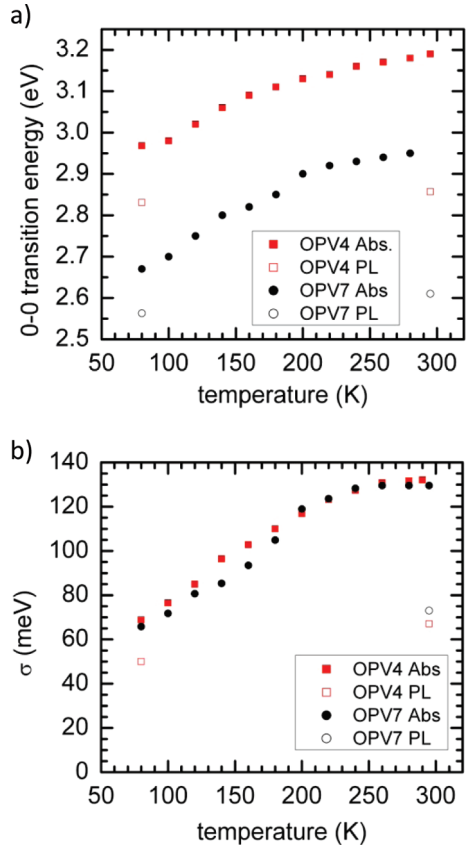

Figure 3. (a) Energy of the $S_1 \leftarrow S_0$ 0−0 transition in absorption and (b) the variance of the Gaussian shaped line width obtained from the Franck−Condon analyses of the spectra for heptyl-OPV4 (filled squares) and heptyl-OPV7 (filled circles) as a function of temperature. Open symbols refer to the $S_1 \rightarrow S_0$ 0−0 transition energy measured in fluorescence.

geneous line broadening. Instead, the absorption spectra are vibrational replicas in which line broadening is comparable to the vibrational splitting so that the spectra become featureless.

Figure 3 shows the so-obtained energy of the $S_1 \leftarrow S_0$ 0−0 transition as well as the variance σ of the Gaussian shaped $S_1 \leftarrow S_0$ 0−0 transition as a function of temperature for two oligomers of different length, heptyl-OPV4 and heptyl-OPV7. It documents that σ decreases by more than a factor of 2 upon cooling near 80 K. By and large, between 100 and 200 K, σ could be approximated by a $\sigma \propto T^{2/3}$ law, recognizing, though, that the actual $\sigma(T)$ dependence is sigmoidal if plotted on a $\log(\sigma)$ versus $\log(T)$ dependence, and it tends to level off above 240 K. This is discussed in more detail further below in the context of Figure 14. In addition to absorption, the same kind of Franck−Condon deconvolution can be applied to the 80 and 290 K fluorescence data of ref 28 to yield the $S_1 \rightarrow S_0$ 0−0 line width and energy indicated in Figure 3. At 290 K, there is a Stokes' shift between the 0−0 transitions of absorption and emission of 330−350 meV. It becomes smaller upon cooling. Since for oligomers in solution of a concentration of 10^{-5} mol/L there can be no energy transfer, this temperature dependent Stokes' shift, which is accompanied by spectral narrowing, must be due to conformational relaxation toward a more planar structure with increased delocalization of the excited singlet state. Site selectively recorded fluorescence spectra at 10 K bear out a residual Stokes' shift of approximately 30 meV.[27] Obviously, there is a finite chain relaxation even in a rigid 10 K MeTHF matrix.

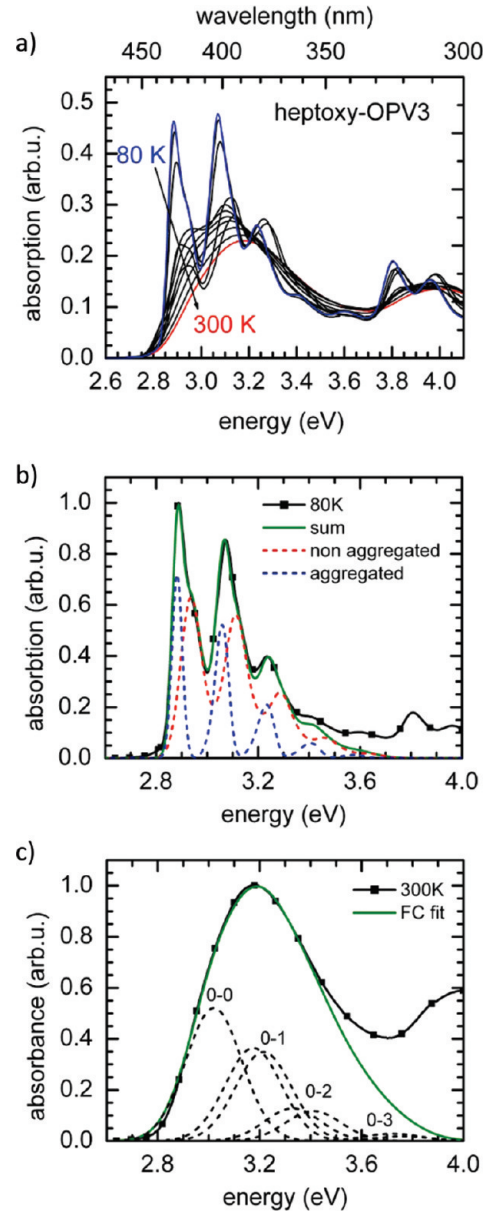

Figure 4. (a) Absorption spectra of heptoxy-OPV3 recorded in a MeTHF solution at different temperatures starting at 300 K in 20 K steps down to 80 K ($c = 4 \times 10^{-5}$ mol/L (from ref 28). (b) Franck−Condon fit (green solid line) to the 80 K spectrum (black line with filled squares) indicating that there is a superposition of the nonaggregated and aggregated oligomers. The Franck−Condon fits to the nonaggregated and aggregated oligomers are shown as blue and red dotted lines, respectively. (c) Franck−Condon analysis (green solid line) of the absorption spectrum (black line with squares) of the nonaggregated oligomer at 300 K. The 0−0 peak and overtones of the two vibrational modes involved are indicated as black dotted lines. For clarity, linear combinations of overtones and higher overtones are omitted in the display, yet included in the fit.

The temperature dependences of the absorption spectra of heptoxy-OPV oligomers shown in Figure 4 are similar, but there are important differences. While at room temperature the absorption spectrum is broad and featureless, a vibrationally well-resolved low energy feature evolves upon cooling. A Franck−Condon analysis of the heptoxy-OPV3 in MeTHF solution at a concentration of 4×10^{-5} mol/L indicates that below 160 K there is aggregation occurring. The absorption spectra are a superposition of the features of aggregated and nonaggregated oligomers. This is exemplified in Figure 4b,c, which show a Franck−Condon analysis of the absorption spectra

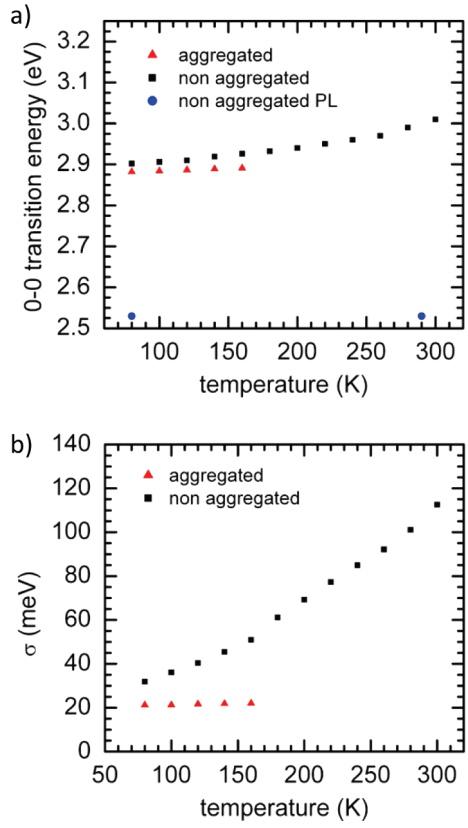

Figure 5. (a) Energy of the $S_1 \leftarrow S_0$ 0−0 transition of aggregated and nonaggregated heptoxy-OPV3 and (b) its line width σ as a function of temperature. Round circles refer to data taken from the fluorescence spectra.

at 80 K and at 290 K. In contrast to the room temperature data, at low temperature, the absorption spectrum cannot be simulated by a single vibrational progression. It requires the two progressions shown to construct the spectrum. The occurrence of aggregation in alkoxy-substituted PPV is well documented.[33,35−39] This is not the focus of this manuscript and will therefore be discussed in more detail elsewhere. For the purpose of understanding the origin of inhomogeneous broadening, we concentrate mainly on the data from the nonaggregated oligomers. The inhomogeneous broadening of the $S_1 \leftarrow S_0$ 0−0 transition of the nonaggregated oligomers bears out superlinear temperature dependence while the σ of the aggregate is as low as 21 meV and independent of temperature (Figure 5). For the following discussion of the results it will be helpful to relate $\sigma(T)$ to the temperature dependent shift of the $S_1 \leftarrow S_0$ 0−0 transition and to compare the dependence of heptyl and heptoxy-substituted compounds (Figure 6). It turns out that the slope, $d\sigma/d\varepsilon$, of the heptoxy-OPV3 is about a factor of 3 larger than that of heptyl-OPV4 and heptyl-OPV7. It is also noteworthy that both the absorption and the fluorescence spectra of the series of the heptoxy compounds are bathochromically shifted to those of the heptyl derivatives. The data for heptyl and heptoxy-substituted OPV4 are listed in Table 1. This red shift of the heptoxy-OPV spectra relative to heptyl-OPV is a reflection of the greater delocalization of the π−electron distribution. It demonstrates that the heptoxy-OPVs are more planar that heptyl-OPV. This is confirmed by density functional calculations on the optimized ground state geometry and excited state geometry in the gas phase for ethyl-OPV4 and methoxy-OPV4 (Figure 7). In combination with the experimentally observed Stokes' shift (vide infra) these DFT calculations indicate that after

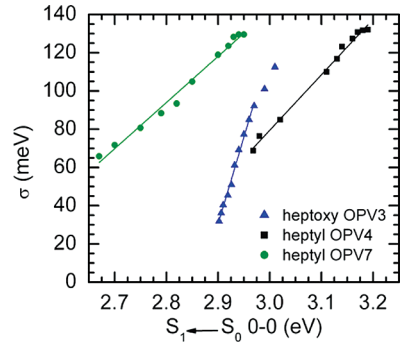

Figure 6. Relation between the variance σ of the inhomogeneous line width for the $S_1 \leftarrow S_0$ 0−0 transition in absorption and the transition energy for heptyl-OPV4, heptyl-OPV7, and heptoxy-OPV3 in MeTHF solution.

TABLE 1: Energies of the S_1−S_0 0−0 Transition of Heptyl-OPV4 and Heptoxy-OPV4 in Absorption and Fluorescence (from Refs 27 and 28)

	heptyl-OPV4		heptoxy-OPV4	
	290 K	80 K	290 K	80 K
$S_1 \leftarrow S_0$ 0−0 (eV)	3.19	2.98	2.73	2.63
$S_1 \rightarrow S_0$ 0−0 (eV)	2.86	2.83	2.57	2.57
Stokes' shift (meV)	330	150	160	60

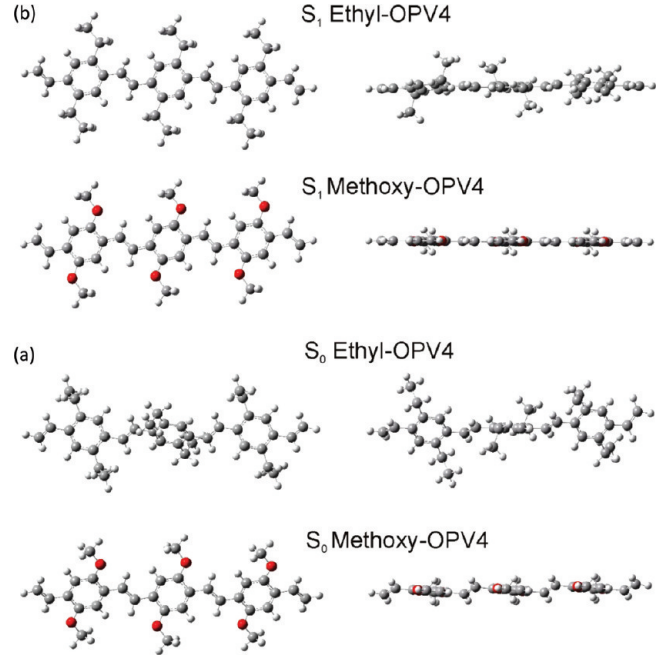

Figure 7. Density functional calculations showing the optimized geometries of ethyl-OPV4 and methoxy-OPV4 (a) in the S_0 ground state and (b) in the S_1 excited state. The oligomers are shown in a top view (left) and a side view (right). The greater planarity of the methoxy-substituted compound is clearly visible.

relaxation the excited state is more delocalized than the initially generated Franck−Condon State.

To relate the behavior of OPV oligomers with the MEH-PPV polymer, we measured the absorption and fluorescence spectra of MEH-PPV in MeTHF solution and of a MEH-PPV film. Like for alkoxy-substituted OPV oligomers, there is also some aggregation phenomenon occurring in MEH-PPV that is manifested in solution absorption spectra below 180 K, or in emission spectra at concentrations at and above 10^{-6} mol/L. To keep the discussion on the inhomogeneous line broadening clear and focused, we only consider data where aggregation

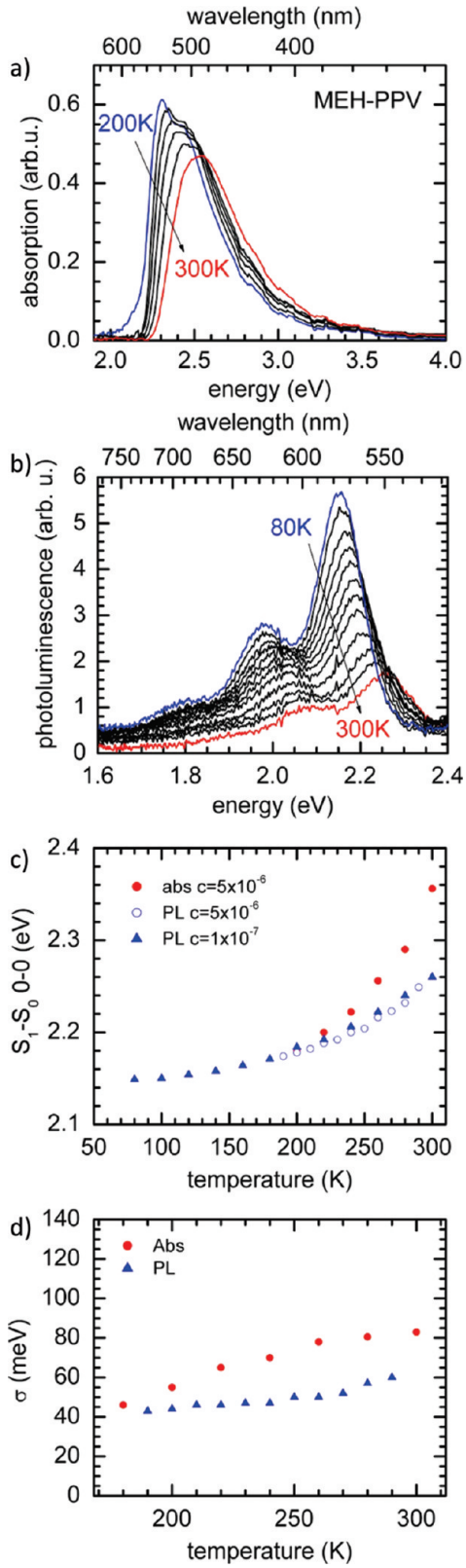

Figure 8. (a) Absorption spectra of nonaggregated MEH-PPV chains in MeTHF solution at a concentration of 5×10^{-6} mol/L between 300 and 200 K. (b) Fluorescence spectra of MEH-PPV spectra in MeTHF solution at a concentration of 1×10^{-7} mol/L within a temperature range 300 to 80 K. (c) and (d) show the peak positions of the S_1-S_0 0−0 transition in absorption and fluorescence and the related variances of the 0−0 lines.

effects are absent. Figure 8a shows the absorption spectra between 300 and 200 K at a concentration of 5×10^{-6} mol/L.

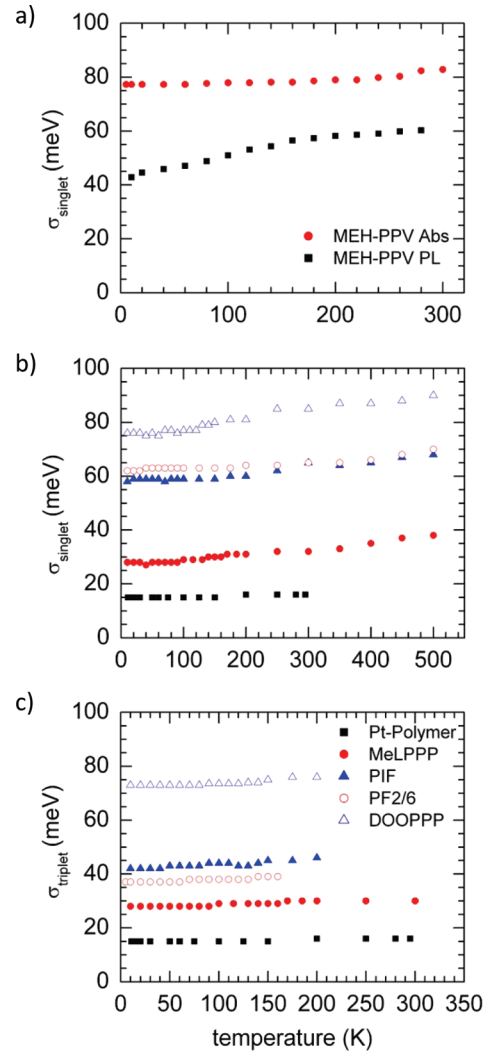

Figure 9. Temperature dependence (a) of the line widths of the S_1-S_0 0−0 transition in absorption and fluorescence of a MEH-PPV film, and (b) of the line widths of the 0−0 transition in fluorescence and (c) in phosphorescence of films of DOO-PPP, PF2/6, PIF, MeLPPP, and the Pt polymer.

Figure 8b depicts the fluorescence spectra between 300 and 80 K at a concentration of 10^{-7} mol/L. The peak positions of the S_1-S_0 0−0 in absorption and fluorescence as well as the bandwidth as a function of temperature are shown in Figure 8c while Figure 8d documents the variances of the $S_1 \rightarrow S_0$ 0−0 transition in absorption and fluorescence. Figure 8c demonstrates that at 300 K there is a Stokes' shift of about 100 meV that decreases continuously and vanishes below 200 K. Within the same temperature interval the gap between the σ values in absorption and fluorescence diminishes. Comparing Figures 3b, 5b, and 8d indicates that, at room temperature, the inhomogeneous line broadening decreases along the series heptyl-OPV, heptoxy-OPV, and MEH-PPV.

After reflecting on the solution data, we now consider how the inhomogeneous broadening changes with temperature if the polymer is in a thin film environment. Figure 9a shows the σ values for the S_1-S_0 0−0 transitions in absorption and fluorescence of a MEH-PPV film as a function of temperature. Figure 9b,c reproduces from ref 29 the σ values of the $S_1 \rightarrow S_0$ 0−0 bands in fluorescence as well as the $T_1 \rightarrow S_0$ 0−0 bands in phosphorescence for films of DOOPPP, PF2/6, PIF, MeLPPP, and Pt polymer.[29] We note that in this order of compounds, the torsional degree of freedom is gradually reduced. Except for

the MEH-PPV fluorescence, the σ values are virtually temperature independent between 10 and 200 K. Only a 10−20% increase is noted upon heating up to 500 K. To compare the line width in films reported in ref 29 with the line width in solution for the rigid polymer MeLPPP, we took measurements in 10^{-7} mol MeTHF solution and applied a Franck−Condon deconvolution to obtain the 0−0 positions and σ. Figure 10 shows that the widths of the S_1-S_0 0−0 transitions in absorption and in emission are, within experimental accuracy, identical for film and solution. This proves that planarity of the chain by covalent bridging among the phenylene rings eliminates the temperature dependent increase of σ and prevents any major conformational relaxation. It also demonstrates that changing the matrix from solution to film has very little effect on the energy of the $S_1 \rightarrow S_0$ 0−0 transition.

4. Discussion

4.1. General Approach. We now proceed to analyze the data presented above with the aim to identify which contribution to the inhomogeneous line broadening arises from torsional displacements on a π-conjugated chain, and which part is caused mainly by the polarization of the environment. To identify the torsional contribution, we will advance as follows.

Naturally, there is no torsional contribution to the inhomogeneous broadening for a planar oligomer or polymer. For nonplanar compounds, torsional displacements of chain elements will introduce conjugation barriers and, in the extreme case, conjugation breaks. This leads to exciton confinement. As a consequence, the length scale over which an optical excitation remains phase coherent becomes less than the molecular length. This length, which will be designated as the effective conjugation length, determines the energy of the excitation and, being a statistical quantity, the energetic inhomogeneity.[40] An essential goal of the following discussion is therefore to determine the effective conjugation length. This is expressed in terms of the effective number of repeat units N_{eff} that establish a chromophore. Since we are dealing with continuous wave spectroscopy we are only interested in disorder that is static on the time scale of the lifetime of a singlet or triplet excitation. In this limit we can extract the inhomogeneous line broadening from the absorption and emission spectra and we can derive N_{eff} by employing a semiempirical relation between the energy of an excitation as a function of chain length. This allows us to compare the difference that arises in the inhomogeneous broadening between a planar oligomer and the "real" oligomer with torsion by plotting the variance as a function of $[(1/N_{eff}) - (1/N)]$. When this functionality is extrapolated to $N = N_{eff}$, the resulting σ value is the contribution that is due to the fully planar system, i.e., the contribution of the Van der Waals coupling of the exciton to its environment. When the contribution from the polarization of the environment has been obtained, the contribution due to the torsion can be derived. We shall recognize, however, that in fluid solutions there can be an additional line broadening if the solvation shells of a chromophore in absorption and emission are different. We further note that this approach does not consider other contributions to disorder such as self-localization that, according to ref18 may reduce the effective conjugation length.

4.2. Determination of the Effective Conjugation Length. To quantify the dependence of the energy of the $S_1 \leftarrow S_0$ 0−0 absorption transition as a function of the chain length, expressed in terms of the number of repeat units N, we adopt the simple exciton model

$$\varepsilon(N) = \varepsilon_0 + 2\beta \cos\left(\frac{\pi}{N-1}\right) \quad (1)$$

where ε_0 is the monomer transition energy and β is the exchange interaction between neighboring monomers.[41−43] To parametrize

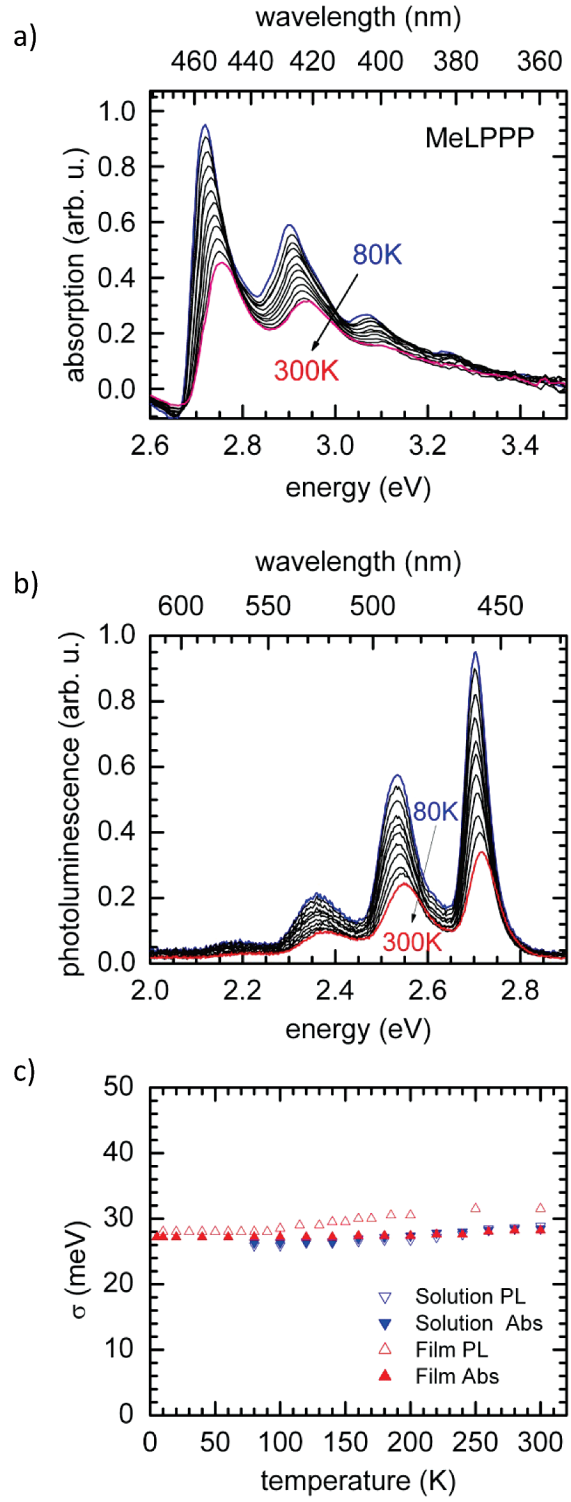

Figure 10. (a) Absorption spectra of MeLPPP polymer in MeTHF solution at a concentration of 10^{-7} mol/L between 300 and 80 K. (b) Fluorescence spectra of MeLPPP in MeTHF solution at a concentration of 10^{-7} mol/L within a temperature range of 300 to 80 K. (c) Comparison of the line widths of the S_1-S_0 0−0 of MeLPPP in MeTHF solution (blue triangles down) and film (red triangle up) measured in both absorption (filled symbols) and fluorescence (open symbols).

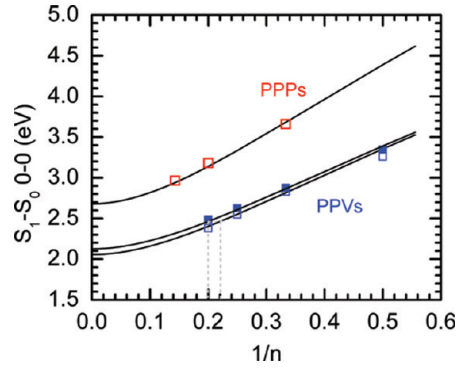

Figure 11. Dependence of the energy of the $S_1 \rightarrow S_0$ 0−0 transition of a PPV chain and a ladder-type poly(*p*-phenylene) chain as a function of the number of the repeat units (open symbols). Fits to eq 1 are indicated as solid lines. In the case of OPV, $N = n + 1$, where n is the number of phenylene vinylene units (see Figure 1); in the case of oligomers of MeLPPP n is the number of phenylene rings. Experimental data for OPV are taken from 80 K fluorescence spectra of heptoxy-OPV,[28] data for MeLPPP-oligomers are taken from the work of Pauck et al.[44] employing the site selection technique in fluorescence at 6 K. For illustration, the energy dependence of the $S_1 \leftarrow S_0$ 0−0 transition is also shown for heptoxy-OPV at 80 K (filled symbols) along with gray guiding lines exemplifying how to derive the effective conjugation length for the case of heptoxy-OPV6.

the $\varepsilon(N)$ dependence, we require data for planar oligomers of the *p*-phenylene family and of the *p*-phenylenevinylene family. In this analysis we take N as the number of phenylene groups within a LPPP oligomer and, for OPVs, $N = n + 1$, where n is the number of phenylenevinylene units. We shall employ $S_1 \rightarrow S_0$ 0−0 fluorescence energies rather than transition energies determined from the absorption maxima since emission takes place from the relaxed and therefore more planar excited state geometry, in particular for the OPVs.

For the oligomers of MeLPPP we use the values of the $S_1 \rightarrow S_0$ 0−0 transition determined by site selective fluorescence spectroscopy.[44] The fit parameters obtained are $\varepsilon_0 = 6.10$ eV and $\beta = -1.71$ eV. This predicts the transition energy of the infinite chain to be at 2.68 eV, in good agreement with the 0−0 fluorescence transition of MeLPPP in MeTHF solution at lower temperatures (2.69 eV) (compare Figures 10a and 11). To parametrize eq 1 for planar OPVs, we chose heptoxy-OPVs as model compounds. Fitting eq 1 to the $S_1 \rightarrow S_0$ 0−0 energies yields $\varepsilon_0 = 4.65$ eV and $\beta = -1.30$ eV (Figure 11). We used heptoxy-OPVs because there is experimentally good reason to assume that upon optical excitation the chain relaxes into a planar structure, implying that the effective conjugation length is identical with the molecular length. This notion is supported by the observations that

(i) the $S_1 \rightarrow S_0$ 0−0 fluorescence transition energies at 80 and 290 K are virtually identical, unlike in heptyl-OPV (see Figures 3 and 5),
(ii) the energy of the S_1-S_0 0−0 transitions in absorption and fluorescence are significantly lower than those of the alkyl-substituted compounds of the same nominal chain length (see Table 1),
(iii) upon site selective spectra recording at low temperatures, the 0−0 transitions in absorption and fluorescence are resonant implying that there is no residual conformational relaxation,[28] and
(iv) quantum chemical calculations indicate that heptoxy-OPV tends to adopt a planar structure even in the ground state, and in particular in the excited state (see Figure 7).

Obviously, the replacement of the heptyl group by the heptoxy group has a planarizing effect on the chain and leads to an extension of the π-electron distribution.[45,46] It is gratifying to note that the $S_1 \rightarrow S_0$ 0−0 emission energies of MEH-PPV oligomers with $n = 3$, 5, and 9 reported by Mirzov[43] are consistent with the data on heptoxy-PPVs reported by Narwark.[27,28] By considering the heptoxy-OPVs at 80 K in emission to be entirely planar and with a fully delocalized π-system, we have thus established a parametrized $\varepsilon(N)$ dependence. We can use this to derive the corresponding shorter effective conjugation length that is associated with the excited state upon absorption, i.e., prior to geometric relaxation. For illustration, the 80 K $S_1 \leftarrow S_0$ absorption energies are indicated in Figure 11. By comparison with the emission energies, N_{eff} can be deduced, as illustrated by the dashed line in Figure 11 for the case of heptoxy-OPV6. The so-derived values for N_{eff} for heptoxy-OPVs are given in Table 2 for 80 and 290 K.

In the same fashion, we now derive the effective conjugation length N_{eff} from the temperature dependent $S_1 \leftarrow S_0$ 0−0 absorption energies of heptyl-OPVs (Figure 3) and MEH-PPV (Figure 8) in fluid solution (Figure 12). The result shows that

(i) the effective conjugation length increases when the temperature is lowered but remains always significantly less than the total oligomer length and
(ii) at temperatures below the glass transition, the maximum effective conjugation length N_{eff} of the alkyl compounds settles at a value of only about $N_{eff} = 4$ (2.9) for a seven-(four-)membered oligomer, i.e., much less than the real chain length.

On passing we note that a Stokes' shift of 330 meV at 290 K for the four-membered heptyl-oligomer (Table 1) indicates

TABLE 2: Energy of the S_1-S_0 Transitions of Heptoxy-OPVs Taken from the Franck−Condon Analysis of the Absorption and from the Fluorescence, along with the Oligomer Length *n* and with the Effective Chain Length N_{eff}[a]

	N_{eff}		$S_1 \rightarrow S_0$ 0−0 (eV)	$S_1 \leftarrow S_0$ 0−0 (eV)	
N	80 K	290 K	80 K	80 K	290 K
2	1.96	1.93	3.27	3.35	3.41
3	2.78	2.74	2.86	2.88	2.93
4	3.58	3.33	2.57	2.63	2.73
5	4.35	3.85	2.35	2.48	2.60
6	5.07	4.25	$(2.32)^{extrapol}$	$(2.38)^{extrapol}$	2.53
7	5.71	4.50	$(2.26)^{extrapol}$	$(2.31)^{extrapol}$	2.49

[a] N_{eff} is inferred from the transition energies in absorption using eq 1, as illustrated in Figure 11.

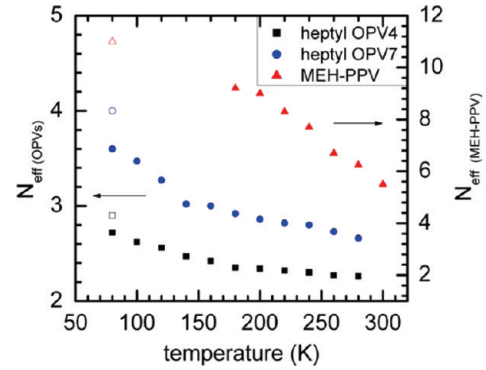

Figure 12. Effective conjugation expressed in terms of the effective number of repeat units N_{eff} as a function of temperatures derived from the inhomogeneous broadening of the $S_1 \leftarrow S_0$ 0−0 absorption line (filled symbols) of heptyl-OPV4, heptyl-OPV7, and nonaggregated MEH-PPV in MeTHF solution. Open symbols refer to values derived from the $S_1 \rightarrow S_0$ 0−0 fluorescence line.

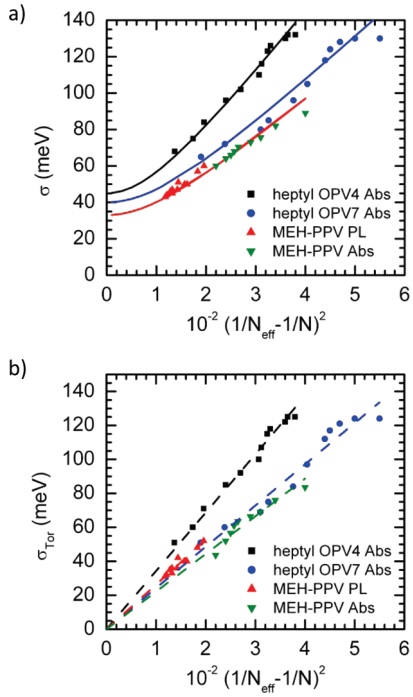

Figure 13. (a) Dependence of σ on $(1/N_{eff} - 1/N)^2$ for heptyl-OPV4, heptyl-OPV7 and MEH-PPV. Solid lines are fits based upon equ. 1. (b) The contribution of σ_{Tor} to the torsional displacements of the chain as a function of $(1/N_{eff} - 1/N)^2$.

that N_{eff} increases from 2.2 to about 3.0 upon optical excitation. Obviously, optical excitation introduces a driving force toward intrachain ordering[45,46] yet is insufficient for complete planarization of the chain. This is at variance with the situation in the alkyloxy OPVs.

4.3. Discrimination of Interchain (Polarization-Induced) and Intrachain (Torsion-Induced) Contributions to Inhomogeneous Broadening. ***(i) Solutions.*** We now consider the variation of σ with N_{eff}. This provides a way to separate the contribution of torsional displacement, σ_{Tor}, and the Van der Waals contribution due to the environment, σ_{VdW}. For a nonplanar oligomer both terms must contribute, but the torsional contribution must vanish when N_{eff} approaches the real chain length, N, and σ_{Tor} must increase the more N_{eff} differs from N. An useful variable is therefore $\Delta(1/N_{eff}) = (1/N_{eff}) - (1/N)$, which is a measure for the difference between the reciprocal *effective* conjugation length and the reciprocal *real* chain length. A large $\Delta(1/N_{eff})$ value implies a chain with strong torsions, while a small one suggests a near planar chain. Empirically, we find that for large $\Delta(1/N_{eff})$, the inhomogeneous broadening σ depends quadratically on the torsional-induced change in the effective chain length, i.e., $\sigma \propto [\Delta(1/N_{eff})]^2$. In Figure 13a, σ is therefore plotted against $[\Delta(1)/(N_{eff})]^2$. Considering that uncorrelated variances of σ_{Tor} and σ_{VdW} add up quadratically, i.e., $\sigma = (\sigma_{Tor}^2 + \sigma_{VdW}^2)^{1/2}$, one can fit the experimental data for heptyl-OPV4 and heptyl-OPV7 by the relation

$$\sigma = \sqrt{c\left(\Delta\frac{1}{N_{eff}}\right)^4 + \sigma_{VdW}^2} \qquad (2)$$

where c is a constant.

The intercept with the ordinate, where effective chain length and real chain length are identical, yields σ_{VdW}. We find σ_{VdW} is 45 meV for heptyl-OPV4 and 40 meV for heptyl-OPV7. Considering that the change in σ_{VdW} with oligomer length is small compared to the overall change in σ with $[\Delta(1/N_{eff})]^2$, we approximate σ_{VdW} to be constant with effective chain length and subtract it from σ according to eq 2 to obtain the torsional contribution σ_{Tor}. Figure 13b shows how σ_{Tor} varies with $[\Delta(1/N_{eff})]^2$.

To analyze the polymer data, the chain is considered to be infinite, i.e., $1/N = 0$. Within experimental accuracy, we find the data for absorption and fluorescence for MEH-PPV polymer in fluid MeTHF solution obey the same relation, and we extrapolate to find σ_{VdW} is 33 meV for MEH-PPV. We note that σ_{VdW} is the same for absorption and fluorescence. This indicates that there is no major reorganization of the solvent shell around the polymer chain upon optical excitation, keeping in mind, though, that minor changes of σ cannot be distinguished because σ - values add up quadratically.

The above data analysis indicates that for the heptyl oligomers and the MEH-PPV polymer in fluid solution the dominant contribution to line broadening is due to torsional intrachain disorder. The situation is opposite for heptoxy-OPVs. In Table 2 the data for the N_{eff} and the ratio of effective chain length to the molecular length for a series of heptoxy-OPVs, measured in absorption, are summarized. For short chains, N_{eff} approaches the real chain length, suggesting a nearly planar chain for the heptoxy-OPVs, in contrast to the heptyl-OPVs. It implies that the torsional contribution to σ has to be small. On the basis of Figure 13b and Table 2, one would expect that for all heptoxy-OPVs, σ_{Tor} is <15 meV with a tendency to decrease toward shorter chains. At room temperature, the experimentally measured values for σ, including both the torsional and environmental contributions are about 115 meV for all heptoxy-OPVs almost independent of oligomer length. This is illustrated in Figure 5 for heptoxy-OPV3 and was derived for the other oligomers using a Franck−Condon analysis for the data published in refs 27 and 28. So, while for the heptyl-OPVs, σ_{Tor} is larger than σ_{VdW}, the converse is the case for the heptoxy-OPVs. We note that the larger Van der Waals contribution in heptoxy-OPVs relative to heptyl-OPV is only present in absorption. When the fluorescence data for heptyl and heptoxy OPVs are considered, σ_{VdW}'s are very similar, that is, 50 ± 10 meV. From this one must conclude that in the case of heptoxy-OPVs the broadening of the $S_1 \leftarrow S_0$ 0−0 absorption is determined by the solvation shell around the chromophore.

From the line broadening of the S_1-S_0 0−0 transition as well as the transition energy, we must conclude that heptyl-OPVs and heptoxy-OPVs are different in several aspects. The fact that the absorption spectra of heptoxy-OPVs are bathochromically shifted relative to the heptyl-OPVs indicates that the former are more extended already in the ground state from which absorption takes place. Consequently, the inhomogeneous broadening must essentially be determined by the chain environment. Upon excitation, the heptoxy-OPVs can relax to the fully elongated conformation while the heptyl-OPVs never attain full planarity, not even in the gas phase (see Figure 7), although their Stokes' shift is larger than that of the heptoxy-OPVs. The larger Stokes' shift is because the heptyl-OPVs may have a less planar ground state geometry, and thus the *relative* increase of the effective conjugation length is larger.

Using Figure 13 and the fact that σ_{Tor} and σ_{VdW} add quadratically, we find that for heptyl-OPVs, σ_{VdW} is virtually the same in absorption and fluorescence. The same analysis can be carried out for heptoxy-OPVs using the data of Narwark et al.[28] It turns out that σ_{VdW} is by about 50% larger in absorption than in fluorescence. This is an interesting side aspect that supports the conclusion that solvation effects are important and

different for the two types of materials. The fact that for the heptyl-OPVs σ_{VdW} is the same in absorption and emission indicates that, in this case, the solvation shell does not change significantly upon excitation in contrast to the heptoxy-OPVs. Apparently, for heptoxy-OPV, the solvent cage becomes more ordered upon excitation. The probable reason is related to the polarity of the heptoxy-pendant groups.

The conclusion that in the heptoxy-OPVs there must be an appreciable change in the solvation cage has an important bearing on the origin of the Stokes' shift as well as on the relation between the S_1-S_0 0−0 transition energy ε and the variance of the line width σ. Recall that in the heptyl-OPVs the variation of σ as a function of temperature is a signature of the temperature-induced variation of the conjugation length N_{eff}. If σ in heptoxy-OPVs is instead determined by σ_{VbW} and, concomitantly, by temperature dependent solvation, the functional dependence of σ versus $\Delta\varepsilon$ must be different for the two materials. This is born out by Figure 6, which shows that the slope of the $\sigma(\varepsilon)$ dependence of heptoxy-OPV3 is 3 times larger than that of heptyl-OPV4 and heptyl-OPV7.

Further, we wish to comment on the magnitude, notably the absence of the Stokes' shift between absorption and fluorescence at 180 K (see Figure 8). The fact that in MEH-PPV both the Stokes' shift vanishes and the variances of the fluorescence and absorption transition bands approach a similar value proves that there is virtually no spectral diffusion. Obviously there is no exciton migration within an isolated polymer chain at $T < 200$ K. Note that randomly excited states within an inhomogeneously broadened density of states distribution must suffer spectral relaxation toward the tail states during their lifetime unless if there is no interstate coupling.[47,48] The absence of a Stokes' shift is therefore evidence that the individual chromophores forming a π-conjugated polymer chain are completely localized. This is consistent with the conclusions of the work of Schwartz inferred from the absence of the decay of optical anisotropy in isolated chains of MEH-PPV.[49] The observed Stokes' shift between absorption and fluorescence in fluid solutions above 200 K can, in principle, be due to energy transfer from shorter to longer chain segments, and/or to conformational relaxation. We favor the latter explanation, because the temperature dependence of the Stokes' shift of MEH-PPV is very similar to that of heptyl- and heptoxy-OPV oligomers in dilute solutions in which energy transfer cannot occur.

(ii) Films. Based upon Figure 11 and the energy of the $S_1 \leftarrow S_0$ 0−0 transition in absorption of a MEH-PPV film (2.14 eV), the effective chain length is $N_{eff} \approx 11$. This implies $[\Delta(1/N_{eff})]^2 \approx 0.01$, which according to Figure 13 translates into a intrachain contribution σ_{Tor} of only about 25 meV. Since the total inhomogeneous width of the $S_1 \leftarrow S_0$ 0−0 transition of the film is as large as 80 meV for all temperatures, the Van der Waals contribution must be $[(80\ \text{meV})^2 - (25\ \text{meV})^2]^{1/2} = 76$ meV. This value has to be compared to that of isolated MEH-PPV chains in solid MeTHF solution, which is only 33 meV (Figure 13a, intersection with the ordinate).

This implies that *in the film* σ is almost entirely controlled by polarization effects due to the environment of the absorbing chain segments rather than the variation of the conjugation length due to torsional displacements of the phenylene groups. We note that is contrary to the situation in fluid solution discussed above. In other words, while in solution the line width of transitions in MEH-PPV is controlled by torsions on the chain, in film it is dominated by the rough energetic landscape of the chain environment. So, σ_{VdW} is highly sensitive to the environment of a chain, as expected. Upon forming a polymer film by spin-coating from solution, inhomogeneous line broadening is largely determined by metastable interchain disorder that is preserved upon solvent evaporation. This difference between solution and film needs to be kept in mind when concluding from the line width about the effect of different solvents on chain conformation.[39,50] This effect of intermolecular order on the line width is reminiscent of the large effect the substrate temperature has on the $S_1 \leftarrow S_0$ 0−0 bandwidth in a vapor deposited amorphous tetracene layer. When the film is deposited onto an 80 K substrate, the variance of the $S_1 \leftarrow S_0$ 0−0 transition energy is about 80 meV. When the substrate temperature is 120 K, the variance reduces to 30 meV.[51,52] This is a signature of temperature-induced structural annealing during film formation.

It is worth noting that while σ for the $S_1 \leftarrow S_0$ 0−0 transition in absorption of the MEH-PPV film is virtually temperature independent, the σ value taken from the fluorescence spectra bears out significant temperature dependence (Figure 9a). It is accompanied by a bathochromic shift of the $S_1 \rightarrow S_0$ 0−0 transition. This is a signature of spectral diffusion of singlet excitons toward tail states of the distribution of singlet states. This disparity regarding the temperature dependences of σ in absorption and fluorescence proves that the spectral narrowing in fluorescence is caused by energy transfer in the MEH-PPV film rather than by freezing out torsional modes.

4.4. Motional Line Narrowing. In addition to this major matrix effect on the inhomogeneous line broadening there are subtle effects observed in both fluid and solid MeTHF solutions. We observe that the line broadening induced by the polarization of the environment, σ_{VdW}, decreases with increasing chain length. For example, from heptyl-OPV4 to heptyl-OPV7, σ_{VdW} decreases from 45 to 40 meV (Figure 13). Similarly, σ_{VdW} for a MEH-PPV chain in solution is about 33 meV (Figure 13) while it is about 115 meV in heptoxy-OPV3, as inferred from analyzing the room temperature solution absorption spectrum (Figure 4). The same trend has been observed in the series of oligomers of MeLPPP to polymer. While σ_{VdW} for the oligomer containing four phenylene rings is 34 meV, it is 26 meV for the polymer, as can be found from considering emission spectra in solution.[44] This effect is reminiscent of motional narrowing in NMR spectroscopy. In a more extended π-conjugated chain, an excited state can explore a larger length scale and is less affected by the rough energy landscape of the environment. This correlates with the fact that intermolecular interactions between chains are weaker as an exciton becomes more delocalized.[16]

4.5. Comparison to the Barford−Trembath Theory. Once we have separated the contribution of static torsional displacements of a chain from the polarization effect of the chain environment, we can determine the temperature dependence of σ_{Tor}. In the theory by Barford and co-workers[18,19] the inhomogeneous line broadening of a poly phenylene chain is attributed to both static torsional disorder and Van der Waals polarization, with both disorder contributions suggested to obey a $\sigma \propto T^{1/2}$ dependence on temperature, resulting in a line width dependence $\propto T^{2/3}$ for absorption. While in the work by Barford and Trembath, the absorption inhomogeneous line width was given to scale as $T^{1/2}$,[18] this was corrected in the subsequent work by Makhov and Barford to be $T^{2/3}$.[19] Figure 14 shows the experimentally derived evolution of σ_{Tor} as a function of temperature for heptyl-OPV4, heptyl-OPV7, and MEH-PPV in solution, along with a dotted line indicating a slope of 2/3. We observe that while σ_{Tor} increases faster than $T^{2/3}$ with a tendency toward saturation near room temperature, the theory gives a good

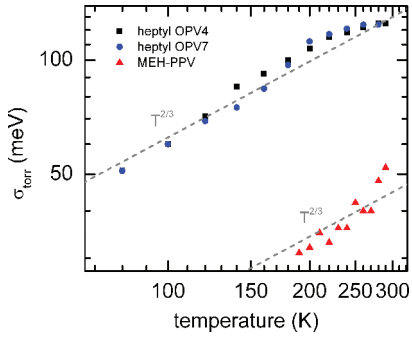

Figure 14. Dependence of the torsional contribution σ_{tor} on the inhomogeneous broadening of the $S_1 \leftarrow S_0$ 0−0 transition in absorption for heptyl-OPV4, heptyl-OPV7, and MEH-PPV. The dashed curve indicates a σ_{Tor} vs $T^{2/3}$ law.

first order approximation for the temperature dependence at moderate temperatures.

In our analysis, we have considered only the disorder effects due to torsion and environmental polarization. Further effects that may cause a reduction in effective conjugation length, as suggested by Barford and Trembath, are considered secondary (since variances add quadratically) and they are not included explicitly. We feel the likely reason for the different evolution with temperature and the different absolute value of σ_{Tor} is that while the theoretical model has a suitable general approach in considering the torsion potential, it is only the (gas phase) intrachain torsional potential of the phenylene rings that is taken into account. In a real world polymer those torsional displacements are impeded by bulky substituents that act as anchors in the molecular environment. This is likely to alter the distribution of possible torsion angles, and therefore the contribution of torsional disorder is diminished as compared to a bare chain, resulting in a different temperature dependence. It is thus important to consider that temperature dependence must be controlled by the collective motion of the chain and its environment. For example, it is obvious that in a solid phase, i.e., in a polymer film or a polymer chain embedded in a glassy matrix, torsional motion is virtually frozen out. This implies that in the film or in a solution below the glass temperature, σ should be more or less temperature independent as it is the case in a system like MeLPPP where major displacements are eliminated by covalent bridging among the phenylene rings. This is confirmed by Figure 9 showing data for a series of polymers. In a theory aimed to describe conjugated polymers used in thin film devices of practical use (as opposed to solutions), such collective effects will need to be included.

In ref 18, the calculated line width due to torsional displacements is estimated to be about 500 meV. Assuming a Gaussian shape this corresponds to a σ_{Tor} of about 220 meV. For the polarization-induced disorder, values in the range of $\sigma_{VdW} = 0.5-1.0$ eV are considered to be realistic estimates of disorder for polymers in hydrocarbon solvents. The experimentally derived values of σ_{Tor} range up to 125 meV for heptyl-OPVs at room temperature (Figure 14). σ_{VdW} is in the range of 40 meV for heptyl-OPV and 115 meV for heptoxy-OPVs at 300 K and decreases to about 50 meV at 80 K. These experimentally found values are significantly lower than the values estimated by Barford and Trembath for the polymer PPP.[18]

4.6. Inhomogeneous Broadening in Singlet versus Triplet Excitations. In this context it is of interest to compare the inhomogeneous line broadening of the 0−0 transitions in fluorescence and phosphorescence. For MeLPPP, the Pt-polymer as well as for DOOPPP the σ values are the same in the singlet and triplet state while in PF2/6 and PIF $\sigma_T/\sigma_s \approx 2/3$ (see Figure 9). When comparing line broadening for singlet and triplet excitations, it is useful first to clarify a few terms. We distinguish between the "size" of the exciton, by which we refer to the mean distance between centers of the electron and hole wave functions, and the conjugation length, by which we mean the number of repeat units over which the exciton moves coherently. We understand this definition of terms is consistent with those used by Barford and Trembath. They further argue that the conjugation length for a triplet exciton be shorter than for a singlet exciton, since the coupling along the chain for triplets (via exchange integrals) be weaker than for singlets. As a result, we would expect that triplets are less susceptible to perturbation by conformational variation such as torsional displacements, and we would intuitively argue that inhomogeneous broadening of phosphorescence lines should be less than that in fluorescence. In contrast, in section II of ref 19. Makhov and Barford argue that the relative disorder is larger for triplets than for singlets by stating that "the disorder being effectively larger for triplets because of their narrower bandwidth", though we note that their theory pertains to absorption only.

Different from this prediction, the present data indicate that the disorder for triplets, expressed through the phosphorescence line width, is smaller than that for singlets, manifested in the fluorescence line width, for compounds such as PF2/6 and PIF. There are also important exceptions of this notion where the line width of fluorescence and phosphorescence are equal. If the main contribution to σ is due to energetic randomness of the chain environment rather than to conformational variation, it should not matter how large the electronic coupling is along the chain because the line inhomogeneity is due to chain environment. MeLPPP and in the Pt-polymer are the most ordered members in the series (as is evident by their narrow line width in absorption and emission), and we consider their σ_T and σ_s values are the same because they are of interchain rather than of intrachain origin. The other extreme is DOO-PPP, which is highly disordered. If an exciton is confined in a short chain segment due to chain disorder, inhomogeneous line broadening should also be the same for singlet and triplet states because in this case the exciton is squeezed by torsional breaks limiting the conjugation and, consequently, the size of the electronic intrachain coupling becomes again irrelevant. The specific localization of triplet excitations should only matter in the case of intermediate disorder, realized, for instance, in PF2/6 and PIF. In this case, the environment-induced interchain and the torsion-induced intrachain disorder are superimposed, yet the intrachain contribution is smaller for triplets than for singlet excitations because triplets are rather more confined. Thus, in summary, there is a difference between the theoretically predicted line width order (with the disorder being larger for the triplets than for the singlet) and the experimentally found result (with an equal or more narrow line width for triplets). This difference may in principle be assigned to the fact that experimental data on a triplet can only be obtained from emission measurements while the theory pertains only to absorption. However, we consider that a dramatic change in the order of the singlet and triplet line width leading to a reversal upon relaxation is unlikely.

5. Conclusions

Stimulated by the current endeavor to understand what effect dynamic and static torsions have on the electronic properties of a π-conjugated chain,[1,18,20−25] we studied the inhomogeneous spectral broadening of singlet excitations in oligomers and

polymers of the poly(*p*-phenylenevinylene)-type and of the poly(*p*-phenylene)-type in fluid and frozen MeTHF solution as well as in bulk films over a broad temperature range. We also compared the inhomogeneous broadenings of fluorescence and phosphorescence spectra in poly(*p*-phenylene)-type films as function of temperature. Using a Franck−Condon analysis to deconvolute the spectra, we determined the temperature dependence of the effective chain length and of the inhomogeneous line broadening. From this information we can distinguish the effect of static intrachain disorder from that of Van der Waals-type polarization in the chain environment and we can extract the temperature dependence of the torsion-induced contribution to the line broadening. By comparing the current experimental results with the recent theory of thermally induced ring torsions by Barford and Trembath, we find that the theory provides insight to the electronic structure of conjugated polymers *in solution*; however, the behavior of materials as used *in thin film* devices is not yet described adequately by the theoretical model. Both the temperature dependence as well as the absolute magnitude of the disorder due to torsional displacements could still be refined. This is particularly true for bulk films of the MEH-PPV and poly(*p*-phenylene)-type materials in which inhomogeneous spectral broadening is virtually temperature independent because conformational disorder is frozen-in when a film is formed from solution. The main reason for the discrepancy between theory and experiment appears to be an insufficient incorporation of effects due to the molecular environment on the torsional motions of the repeat units, such as a higher viscosity due to side chain entanglements. By comparing fluorescence and phosphorescence line widths in poly(*p*-phenylene)-type films we further demonstrate that singlet and triplet line widths can be identical in cases of very small and very high disorder, yet that for intermediate disorder, the phosphorescence line width is smaller than the fluorescence line width. The fact that triplet states are more localized than singlets is only relevant to the line width in the case of intermediate disorder.

In summary, we have established quantitatively how the static intrachain and interchain contributions to inhomogeneous line broadening evolve with temperature both in fluid and in solid systems, for both singlets and triplets. We believe this may provide a useful basis for the interpretations of charge and energy transfer processes that involve chain dynamics, and that this may hopefully stimulate further theoretical endeavors toward a realistic description on the causes and effects of static disorder.

Acknowledgment. We thank SCJ Meskers for supplying the data of Refs 27 and 28 in electronic form. The MeLPPP was supplied by Ulrich Scherf. This work was supported by the German-Israeli Foundation for Scientific Research & Development (GIF) Contract No. I-897-221.10/2005.

References and Notes

(1) Scholes, G. D. *Annu. Rev. Phys. Chem.* **2003**, *54*, 57.
(2) Coropceanu, V.; Cornil, J.; da Silva, D. A.; Olivier, Y.; Silbey, R.; Brédas, J. L. *Chem Rev* **2007**, *107*, 926.
(3) Beenken, W. J. D. *Phys. Status Solidi A-Appl. Mater. Sci.* **2009**, *206*, 2750.
(4) Kador, L. *J. Chem. Phys.* **1991**, *95*, 5574.
(5) Dieckmann, A.; Bässler, H.; Borsenberger, P. M. *J. Chem. Phys.* **1993**, *99*, 8136.
(6) Young, R. H. *Philos. Mag. B* **1995**, *72*, 435.
(7) Novikov, S. V.; Dunlap, D. H.; Kenkre, V. M.; Parris, P. E.; Vannikov, A. V. *Phys. Rev. Lett.* **1998**, *81*, 4472.
(8) Bässler, H. *Phys. Status Solidi B* **1993**, *175*, 15.
(9) Schein, L. B.; Tyutnev, A. *J. Phys. Chem. C* **2008**, *112*, 7295.
(10) Borsenberger, P. M.; Weiss, D. S. *Organic Photoreceptors for Xerography*; New York, NY, U.S., 1998.
(11) Richert, R. *J. Chem. Phys.* **2000**, *113*, 8404.
(12) Cornil, J.; dos Santos, D. A.; Crispin, X.; Silbey, R.; Brédas, J. L. *J. Am. Chem. Soc.* **1998**, *120*, 1289.
(13) Scholes, G. D.; Larsen, D. S.; Fleming, G. R.; Rumbles, G.; Burn, P. L. *Phys. Rev. B* **2000**, *61*, 13670.
(14) Meskers, S. C. J.; Hubner, J.; Oestreich, M.; Bässler, H. *J. Phys. Chem. B* **2001**, *105*, 9139.
(15) Walter, M. J.; Lupton, J. M. *Phys. Rev. Lett.* **2009**, *103*, 167401.
(16) Gierschner, J.; Cornil, J.; Egelhaaf, H. J. *Adv. Mater.* **2007**, *19*, 173.
(17) Brédas, J. L.; Silbey, R. *Science* **2009**, *323*, 348.
(18) Barford, W.; Trembath, D. *Phys. Rev. B* **2009**, *80*, 165418.
(19) Makhov, D. V.; Barford, W. *Phys. Rev. B* **2010**, *81*, 165201.
(20) Milota, F.; Sperling, J.; Szocs, V.; Tortschanoff, A.; Kauffmann, H. F. *J. Chem. Phys.* **2004**, *120*, 9870.
(21) Westenhoff, S.; Beenken, W. J. D.; Friend, R. H.; Greenham, N. C.; Yartsev, A.; Sundström, V. *Phys. Rev. Lett.* **2006**, *97*, 166804.
(22) Schmid, S. A.; Abbel, R.; Schenning, A. P. H. J.; Meijer, E. W.; Herz, L. M. *Phys. Rev. B* **2010**, *81*, 085438.
(23) Chang, M. H.; Hoffmann, M.; Anderson, H. L.; Herz, L. M. *J. Am. Chem. Soc.* **2008**, *130*, 10171.
(24) Cirmi, G.; Brida, D.; Gambetta, A.; Piacenza, M.; Della Sala, F.; Favaretto, L.; Cerullo, G.; Lanzani, G. *Phys. Chem. Chem. Phys.* **2010**, *12*, 7917.
(25) Dykstra, T. E.; Hennebicq, E.; Beljonne, D.; Gierschner, J.; Claudio, G.; Bittner, E. R.; Knoester, J.; Scholes, G. D. *J. Phys. Chem. B* **2009**, *113*, 656.
(26) Rissler, J. *Chem. Phys. Lett.* **2004**, *395*, 92.
(27) Narwark, O.; Gerhard, A.; Meskers, S. C. J.; Brocke, S.; Thorn-Csanyi, E.; Bässler, H. *Chem. Phys.* **2003**, *294*, 17.
(28) Narwark, O.; Meskers, S. C. J.; Peetz, R.; Thorn-Csanyi, E.; Bässler, H. *Chem. Phys.* **2003**, *294*, 1.
(29) Hoffmann, S. T.; Koenen, J.-M.; Forster, M.; Scherf, U.; Scheler, E.; Strohriegl, P.; Bässler, H.; Köhler, A. *Phys. Rev. B* **2010**, *81*, 115103.
(30) Scherf, U.; Müllen, K. *Makromol. Chem., Rapid Commun.* **1991**, *12*, 489.
(31) Khan, A. L. T.; Sreearunothai, P.; Herz, L. M.; Banach, M. J.; Köhler, A. *Phys. Rev. B* **2004**, *69*, 085201.
(32) Khan, A. L. T.; Banach, M. J.; Köhler, A. *Synth. Met.* **2003**, *139*, 905.
(33) Ho, P. K. H.; Kim, J. S.; Tessler, N.; Friend, R. H. *J. Chem. Phys.* **2001**, *115*, 2709.
(34) Khan, A. L. T. Ph.D. thesis, University of Cambridge, 2005.
(35) Sherwood, G. A.; Cheng, R.; Smith, T. M.; Werner, J. H.; Shreve, A. P.; Peteanu, L. A.; Wildeman, J. *J. Phys. Chem. C* **2009**, *113*, 18851.
(36) Traiphol, R.; Charoenthai, N. *Synth. Met.* **2008**, *158*, 135.
(37) Padmanaban, G.; Ramakrishnan, S. *J. Phys. Chem. B* **2004**, *108*, 14933.
(38) Meskers, S. C. J.; Janssen, R. A. J.; Haverkort, J. E. M.; Wolter, J. H. *Chem. Phys.* **2000**, *260*, 415.
(39) Traiphol, R.; Sanguansat, P.; Srikhirin, T.; Kerdcharoen, T.; Osotchan, T. *Macromolecules* **2006**, *39*, 1165.
(40) Bässler, H.; Schweitzer, B. *Acc. Chem. Res.* **1999**, *32*, 173.
(41) Tilgner, A.; Trommsdorff, H. P.; Zeigler, J. M.; Hochstrasser, R. M. *J. Chem. Phys.* **1992**, *96*, 781.
(42) Chang, R.; Hsu, J. H.; Fann, W. S.; Yu, J.; Lin, S. H.; Lee, Y. Z.; Chen, S. A. *Chem. Phys. Lett.* **2000**, *317*, 153.
(43) Mirzov, O.; Scheblykin, I. G. *Phys. Chem. Chem. Phys.* **2006**, *8*, 5569.
(44) Pauck, T.; Bässler, H.; Grimme, J.; Scherf, U.; Müllen, K. *Chem. Phys.* **1996**, *210*, 219.
(45) Di Paolo, R. E.; Burrows, H. D.; Morgado, J.; Macanita, A. L. *ChemPhysChem* **2009**, *10*, 448.
(46) Di Paolo, R. E.; de Melo, J. S.; Pina, J.; Burrows, H. D.; Morgado, J.; Macanita, A. L. *ChemPhysChem* **2007**, *8*, 2657.
(47) Movaghar, B.; Grünewald, M.; Ries, B.; Bässler, H.; Wurtz, D. *Phys. Rev. B* **1986**, *33*, 5545.
(48) Hoffmann, S. T.; Koenen, J.-M.; Forster, M.; Scherf, U.; Scheler, E.; Strohriegl, P.; Bässler, H.; Köhler, A. *Phys. Rev. B* **2010**, *81*, 165208.
(49) Schwartz, B. J. *Annu. Rev. Phys. Chem.* **2003**, *54*, 141.
(50) Aharon, E.; Breuer, S.; Jaiser, F.; Köhler, A.; Frey, G. L. *ChemPhysChem* **2008**, *9*, 1430.
(51) Hesse, R.; Hofberger, W.; Bässler, H. *Chem. Phys.* **1980**, *49*, 201.
(52) Jankowiak, R.; Rockwitz, K. D.; Bässler, H. *J. Phys. Chem.* **1983**, *87*, 552.

JP107357Y